CLM-P313

This document is intended for publication in a journal, and is made available on the understanding that extracts or references will not be published prior to publication of the original, without the consent of the authors.

CULHAM LABORATORY
LIBRARY
21 NOV 1972
6

UKAEA RESEARCH GROUP

Preprint

ELECTRODE HEAT DISSIPATION LIMITS ON MULTI-APERTURE ION SOURCE PERFORMANCE

H C COLE
D P HAMMOND
E M JONES
A C RIVIERE
J SHEFFIELD

CULHAM LABORATORY
Abingdon Berkshire

1972

Enquiries about copyright and reproduction should be addressed to the
Librarian, UKAEA, Culham Laboratory, Abingdon, Berkshire, England

ELECTRODE HEAT DISSIPATION LIMITS ON MULTI-APERTURE ION SOURCE PERFORMANCE

by

H. C. Cole
D. P. Hammond
E. M. Jones
A. C. Riviere
J. Sheffield

(To be submitted for publication in Nuclear Fusion)

A B S T R A C T

The dissipation of heat in the electrodes of multi-aperture ion sources is a major factor in limiting the power output and beam pulse duration. The results of a series of tests on multi-aperture and single aperture arrays are used as the basis for the derivation of formulae which define the limits of the practical operating regime for a single edge cooled electrode element.

U.K.A.E.A. Research Group
Culham Laboratory,
Abingdon,
Berks.

August 1972 (JC)

1. INTRODUCTION

Ion sources with multi-aperture electrodes are now working with pulsed hydrogen ion beam currents of a few amps and at power levels in the 100 kW regime[1,4]. Intense beams of neutral hydrogen atoms, formed when the ion beam is passed through a hydrogen gas neutralizer, are proposed as a means of heating plasma in controlled fusion experiments. In the near future we will require for this purpose ion sources operating in the megawatt regime. We investigate below, for electrodes with multiple circular apertures, the limitations which are placed on the extracted power density by electrode heating problems. The extraction geometry is shown in Figure 1. The analysis is formulated around the following basic points which have emerged from experimental work at Culham Laboratory[1,2].

(a) Our tests show that for multiple circular aperture systems ~1% of the beam power is dissipated in each electrode.

(b) As a result of this heating the electrodes expand. To prevent buckling and consequent increased interception of the beam we curve the electrodes slightly towards the plasma source. The effect of the heating is now to increase the degree of curvature.

(c) We take as a maximum acceptable curvature the level at which the angle subtended by the curved electrodes has risen to the order of the natural beam divergence (~3°) of the individual beams. Experimental observations with different curvature electrodes confirm this as a sensible choice.

(d) These restrictions limit the permitted temperature rise to ~100 K. We calculate the change in temperature with time of a uniformly heated, edge cooled, multi-aperture disk electrode. Two time regimes are identified. For pulse durations (τ) less than the thermal diffusion time (t_{cr}), thermal inertia prevents cooling of the centre of the electrode, the temperature rises linearly with time and for a given beam power we must then limit the pulse duration. For $\tau > t_{cr}$ we are limited by the conduction of power to the edges to a power level at which we are in equilibrium at the maximum permitted temperature rise.

The purpose of this calculation is to establish the safe operating conditions for simple edge cooled extraction electrodes and for combinations of them, on the basis of what is currently achievable. If a source requirement clearly falls well outside the safe region then this indicates that either we must go to a different electrode design, e.g. rectangular slits formed from cooling pipes, or multiple acceleration stage systems, or we must use some clever electrode mount that compensates for the expansion; or we must take more than average precautions to reduce the interception of the beam. As to whether our limits are realistic, we can only say that in situations where we have clearly exceeded these limits we have destroyed the electrodes.

2. POWER DISSIPATION IN THE ELECTRODES

Power is dissipated in the electrodes as a result of positive ions hitting the negative and earth electrodes. These ions release secondary electrons which in the case of the negative electrode are accelerated back towards the plasma source. Some of these secondaries hit the positive elec-

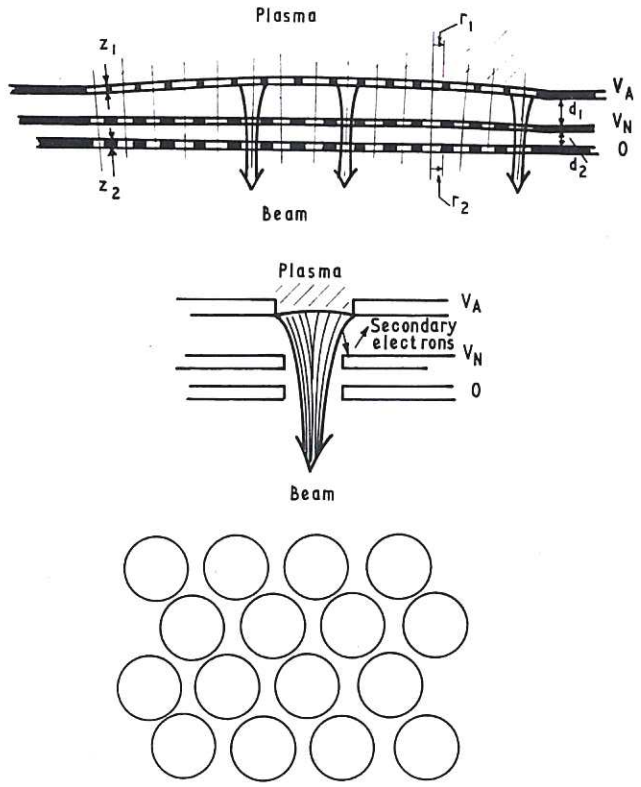

Fig.1 Extraction geometry

trode, and in addition this electrode is heated by the plasma source.

Negative Electrode

The current flowing in the negative electrode circuit is typically ⩽ 3% of the ion beam current (I_B). The fraction $\frac{1}{1+\gamma}$ of this current represents positive ions which hit this electrode at the full acceleration potential ($V_A + |V_N|$), (see Figure 1), γ is the secondary electron coefficient. Now typically $\gamma \sim 2$, and therefore the power dissipated in this negative electrode (W_N) is given by

$$W_N \leqslant 10^{-2}\ W_B \qquad ..(1)$$

where $W_B = I_B V_A$ is the total ion beam power (we take $|V_N| << V_A$).

Positive Electrode

Some of the secondary electrons will hit the acceleration electrode. From the potential profiles plotted in Figure 2 we see that the number will be very small if the plasma-vacuum boundary has a good extraction shape. In practice it is difficult to guarantee perfect plasma illumination of this electrode and the distorted potential profiles in the presence of an undesirably shaped plasma boundary will increase the interception of secondaries. The precise level is hard to assess and for the moment we point out that the intercepted current of secondaries will be ⩽2% of the beam current. We will arbitrarily assume 0.5% interception.

The extraction electrode is also heated by the source. The source current which hits the electrode is $I_s \sim \frac{A}{N\pi r_1^2} \cdot I_B$, where (A) is the surface area of the electrode, we assume that this is uniformly illuminated. The total metal area under optimum extraction conditions when the plasma boundary is right through the electrode is

$$A = \pi a^2 - N\pi r_1^2 + N2\pi r_1 z_1 . \qquad ..(2)$$

There are (N) apertures of radius (r_1) the electrode has a thickness (z_1), the electrode radius is (a). The packing fraction, (transparency) is $P = \frac{Nr_1^2}{a^2}$. It is the level of plasma dissipation on the sides of the aperture that causes us to limit the thickness of the electrode. The maximum possible potential available to drive this source plasma current is somewhere between the source voltage V_s and the sheath potential $\sim 3Te$.

In total for the positive acceleration electrode, we have approximately

$$W_p \leqslant \left[2 \times 10^{-2} + \frac{(1-P)}{P} + \frac{2z}{r_i}\frac{V_s}{V_A}\right] W_B . \qquad ..(3)$$

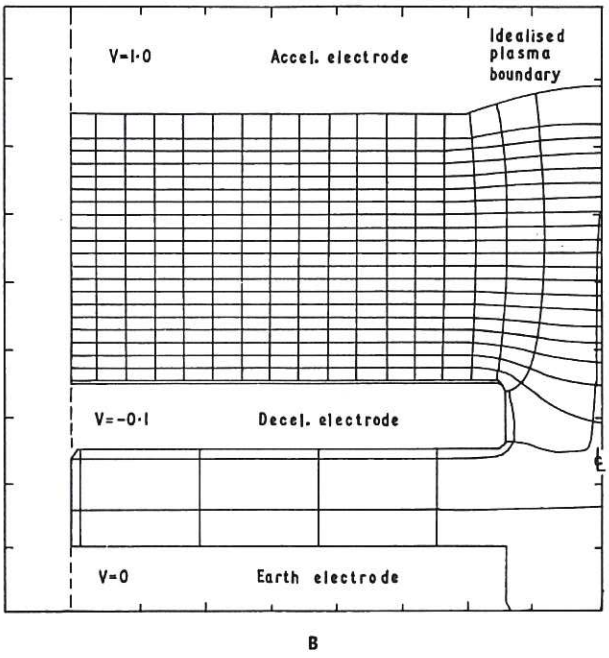

Fig.2 Potential profiles for a single aperture extraction system

Typically $P \sim 0.5 \frac{z_1}{r_1} \sim 1$ and for example $V_s \sim 100$ V, $3T_e \sim 20$ V, $V_A \sim 2 \times 10^4$ V therefore at a minimum.

$$\left\{\frac{(1-P)}{P} + \frac{2z}{r_1}\right\} \frac{3Te}{V_A} \sim 0.3 \times 10^{-2}$$

and with our assumed interception of 0.05% of the beam

$$W_P \leq 10^{-2} W_B \quad .. (4)$$

One final comment, we have neglected the dissipation of radiation from the filament, and we must design the plasma source so that this does not present a problem.

Earth Electrode

The earth electrode and support structure draw a small positive current[2]. It is considered that the current comes partly from slow positive ions and electrons from the neutralisation region, with an excess of the former, and partly from interception of some fast beam ions for which we must include a secondary electron contribution. The current of the latter contribution increases as the aperture diameter decreases and is typically 0.5 mA in a 15 mA beam. The fast ions have the energy V_A and the heat dissipation is therefore

$\frac{1}{(1+\gamma)} \frac{0.5}{15} W_B$. We again take $\gamma \sim 2$ and obtain

$$W_E \lesssim 10^{-2} W_B. \quad .. (5)$$

From (1), (4) and (5) we see that similar fractions of the beam power are dissipated in each electrode and we set the power dissipation

$$W_D = FW_B \quad .. (6)$$

where typically $F \lesssim 10^{-2}$.

3. PEAK ELECTRODE TEMPERATURE

The temperature of a given electrode increases with time as power is dissipated in it until an equilibrium is reached with the conduction of power away from it. We will consider the case of a thin edge cooled disk of radius (a). Clearly most types of electrode structure can be approximated by a group of such disks, where (a) then represents the maximum distance from any part of the electrode to a cooled region.

The temperature profile in a uniformly heated thin disk is given by Carslaw and Jaeger[3] as

$$\Delta T = T - T_o = \frac{H(a^2 - r^2)}{4K} - \frac{2H}{aK} \sum_{n=1}^{\infty} \exp\left[-\left(\frac{K\alpha_n^2 t}{\rho C_v a^2}\right)\right] \cdot \frac{J_o(\alpha_n r)}{\alpha_n^3 J_1(\alpha_n a)} \quad .. (7)$$

where heat is dissipated at the rate of H calories $cm^{-3} sec^{-1}$ for $t > 0$, and (α_n) are the positive roots of $J_o(\alpha a) = 0$, $(a\alpha_1) = 2.4$ etc, (r) is the radial position. The thermal conductivity is K cals $cm^{-1} sec^{-1} K^{-1}$. The density is (ρ) gm cm^{-3}, the specific heat is C_v cal $gm^{-1} K^{-1}$.

We are considering a perforated electrode (see Figure 1) for which the mean electrode density is

$$\rho^* = (1-P)\rho \quad .. (8)$$

The conduction path is also modified and we must make a correction to the conductivity we denote the effective conductivity by

$$K^* = DK \quad .. (9)$$

We have computed the heat flow in a disk perforated with circular apertures in a triangular array and the computed values of D are shown in Figure 3.

The normalized temperature rise at the centre of the disk ΔT_c is plotted as a

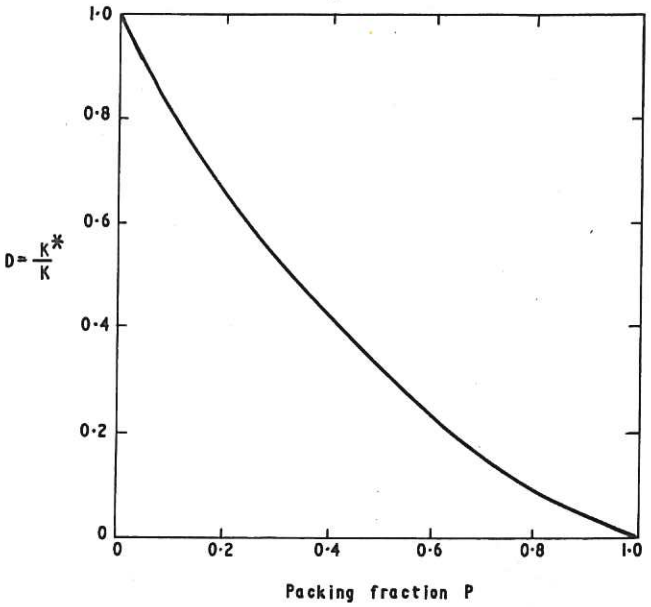

Fig. 3 Thermal conductivity correction factor for a triangular array of circular apertures.

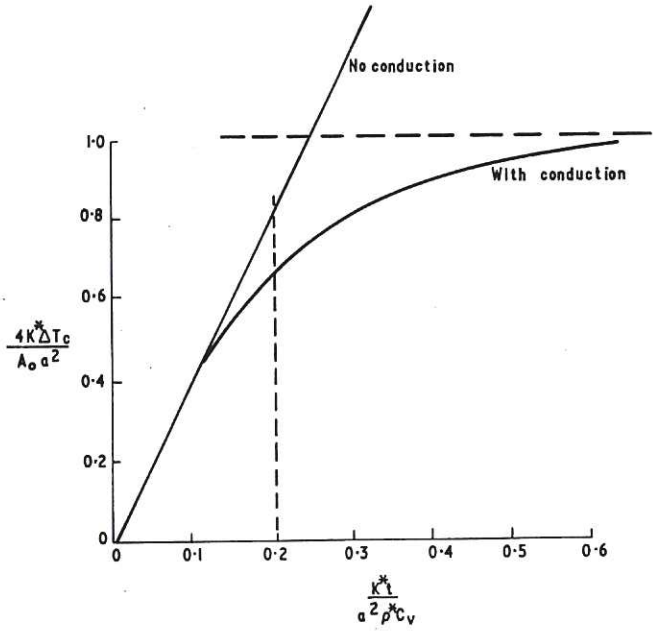

Fig. 4 Time dependence of the normalised temperature at the centre of an edge cooled, uniformly heated disk.

function of the normalized time in Fig.4. It can be seen that the centre temperature is essentially unaffected by conduction for short times τ such that

$$\tau < t_{cr} \equiv \frac{0.2\rho^* C_v a^2}{K^*} \quad . \qquad ..(10)$$

This quantity is plotted for P = 0.5 for copper and molybdenum electrodes in Fig.5. Many ion sources work in this regime where the centre is not cooled during beam extraction and

$$\Delta T_c = \frac{W_D \tau}{4.2\pi a^2 z(1-P)\rho^* C_v} \qquad ..(11)$$

z is the thickness of the electrod.

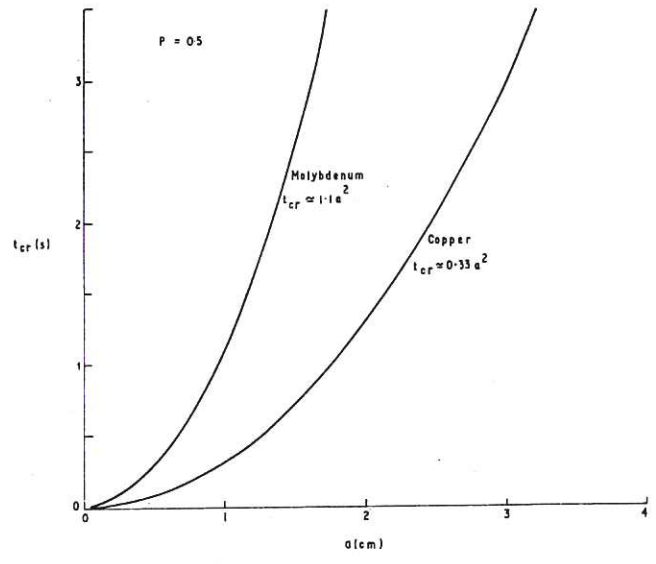

Fig. 5 The critical conduction time as a function of electrode radius

For $\tau > t_{cr}$ with perfect edge cooling

$$\Delta T_c = \frac{A_o a^2}{4K^*} = \frac{W_D}{4\pi z(1-P)4.2K^*} = \frac{W_D t_{cr}}{0.8\rho^* C_v 4.2\pi a^2 z} \quad . \qquad ..(12)$$

4. ELECTRODE CURVATURE

The heat dissipation leads to a differential expansion of the electrode. If the electrode is flat and rigidly held at the edge it will buckle because this is an unstable situation. This will lead to an increased interception of the beam and the electrode will be destroyed. For this reason and also because it helps to focus the beam[1] we curve the electrodes convex to the plasma source. Now as the electrode is heated the curvature increases. Let (x) be the deflection of the centre of the electodes (see Fig.6), the radius of the curvature is

$$R \simeq \frac{a^2}{2x} \quad . \qquad ..(13)$$

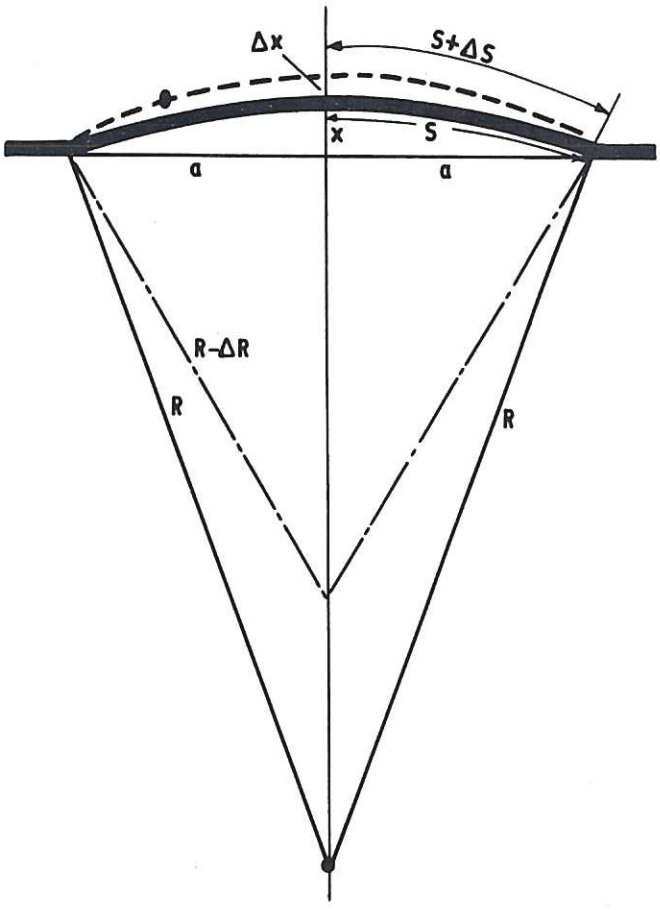

Fig. 6 The change of radius of curvature of a disk with deflection of the centre.

Let (S) be the half circumferential distance. We change this by heating to S + dS, where for the temperature distribution of equation (7)

$$\frac{dS}{S} \simeq \frac{2}{3}\lambda.\Delta T_c \qquad ..(14)$$

and (λ) is the linear coefficient of expansion.

If we start with very small initial deflection of the electrode centre,

$$x \simeq a(\lambda \Delta T_c)^{\frac{1}{2}} . \qquad ..(15)$$

Now the half angle subtended by the electrode is $\theta \simeq \frac{2x}{a}$ and if we limit this to the natural beam divergence of the individual beams ($\theta \lesssim 3.2°$) then we find a maximum allowed temperature of

$$\Delta T_{cm} = \frac{x^2}{a^2\lambda} . \qquad ..(16)$$

For copper $\lambda \simeq 1.5\times10^{-5}$ $\Delta T_{cm} = 60K$.

For molybdenum $\lambda \simeq 0.6\times10^{-5}$ $\Delta T_{cm} = 140K$.

This limit is consistent with the results of tests on the effect of curvature on the beam properties undertaken in reference (1). A deflection of x = 0.1 cm, for a = 3.5 cm ($\theta = 3.2°$) gave a well collimated beam. While overconvergence was obtained with x = 0.25 cm ($\theta = 8°$).

5. THE LIMITATIONS ON THE PERFORMANCE OF A MULTI-APERTURE SOURCE

(a) We are now in a position to determine the maximum permissible beam power W_m, for a given pulse duration τ . In section (3) we estimated that the percentage of the beam power which was dissipated in each electrode was $W_D \sim 10^{-2} W_B$. We will consider the case of the positive electrode to estimate the limitations imposed by heat dissipation.

$\tau < t_{cr}$, with the aid of equations (6) and (11)

$$\frac{Wm}{\pi a^2} \leq \frac{4.2\, z_1(1-P)\rho^* C_v \Delta T_{cm}}{F\tau} \text{ Watts cm}^{-2} \qquad ..(17)$$

z_1 is the electrode thickness.

$\tau > t_{cr}$ with perfect edge cooling, from (6) and (12)

$$Wm \leq \frac{4\pi z_1(1-P)4.2K^*\Delta T_{cm}}{F} \text{ Watts} . \qquad ..(18)$$

(b) The power density which it is possible to extract obeys the law

$$\frac{W}{\pi a^2} \simeq \frac{C_m P V_A^{\frac{5}{2}}}{d_1^2} \text{ Watts cm}^{-2} \qquad ..(19)$$

where ($d_1$cm) is the extraction gap separation.

C_m is the perveance constant. Experimentally for a hydrogen beam[1,2] we find

$$C_m \simeq 2 \times 10^{-8} \text{ Amp(Volt)}^{-\frac{3}{2}} . \qquad ..(20)$$

The maximum power, for a given gap separation is obtained at the breakdown voltage and this is given by[1,2]

$$V_B \simeq 6 \times 10^4 [d_1(\text{cm})]^{\frac{1}{2}} \text{ Volts} . \qquad ..(21)$$

(c) In reference (2) optimum values have been obtained for extraction parameters

$$\varepsilon \equiv \frac{r_1}{d_1} \sim 0.5 \text{ and } \frac{z_1}{r_1} \equiv \beta \sim 0.9 . \qquad .. (22)$$

It is informative to plot the permissible operating power versus V_B while keeping ε, β and P constant, in which case $z_1 = \frac{\varepsilon\beta V_B^2}{B^2}$ . ..(23)

(d) To illustrate the significance of these we plot $\frac{w}{\pi a^2}$ vs V_B ($\tau < t_{cr}$) using equations (17) and (21) in Figure 7, for different (τ), for the typical values $\varepsilon = 0.5$ $\beta = 0.9$, P = 0.5, $F = 10^{-2}$. We are working at the maximum permitted temperature rise. Also plotted is the maximum possible extracted power density, (19), (20) (21),

$$\frac{w_B}{\pi a^2} \simeq \frac{C_m P B^4}{V_B^{\frac{3}{2}}} \text{ Watts cm}^{-2} . \qquad ..(24)$$

We see that for the lower extraction voltages ($V_B \sim$ 10 kV) we are limited mainly by dissipation problems, if we scale the electrode thickness using equation (23). This region we can gain for the longer pulse durations by setting the gap (d_1) wider than we need for the given operating voltage, to take advantage of the good perveance characteristics; this then allows us to use thicker electrodes while maintaining a desirable extraction geometry[2].

Optimum conditions are obtained by equating equations (17) (19) and (22) and

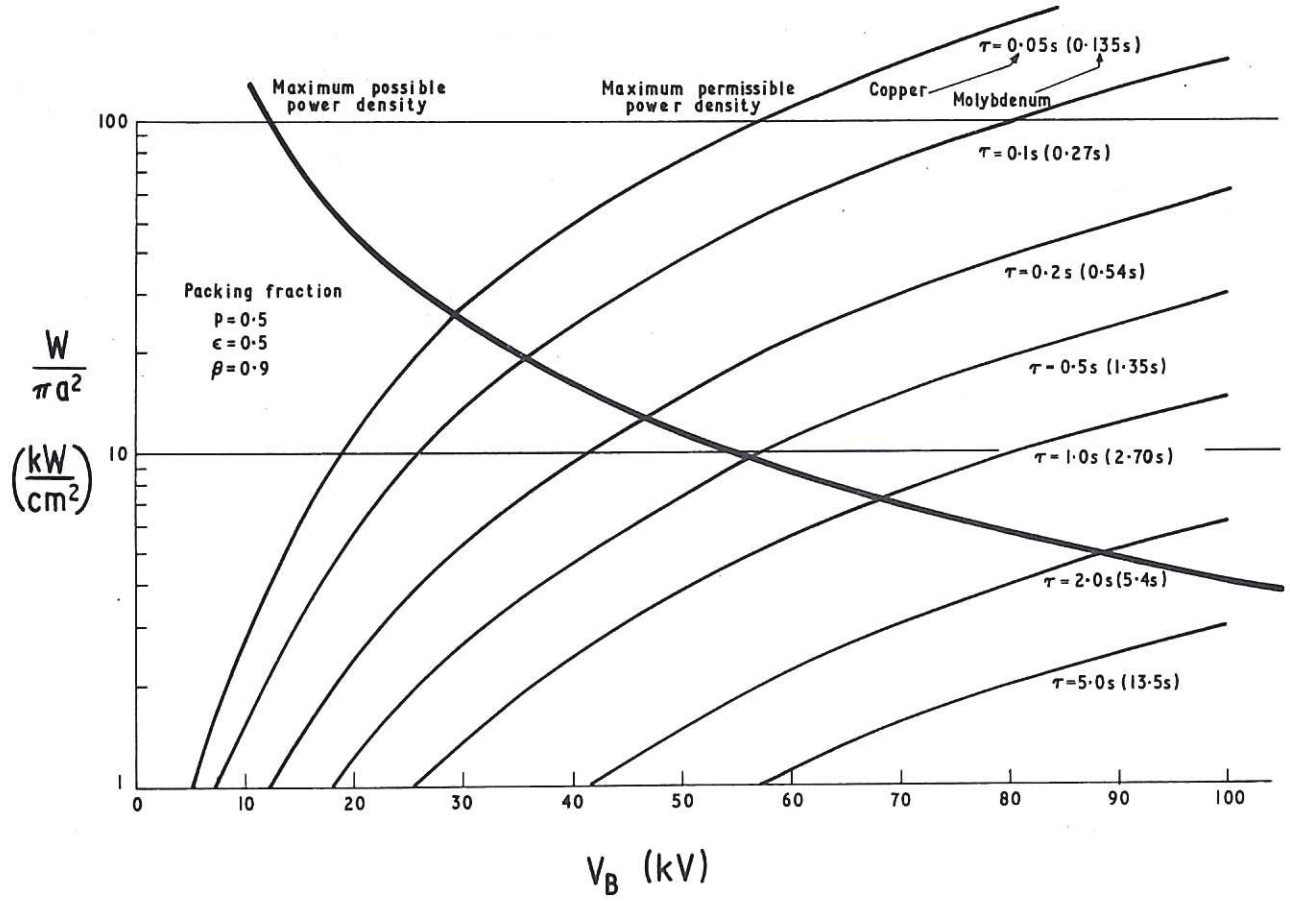

Fig. 7 The limitations on extracted power densities for $\tau < t_{cr}$ as a function of the breakdown voltage (extraction geometry scaled with V_B).

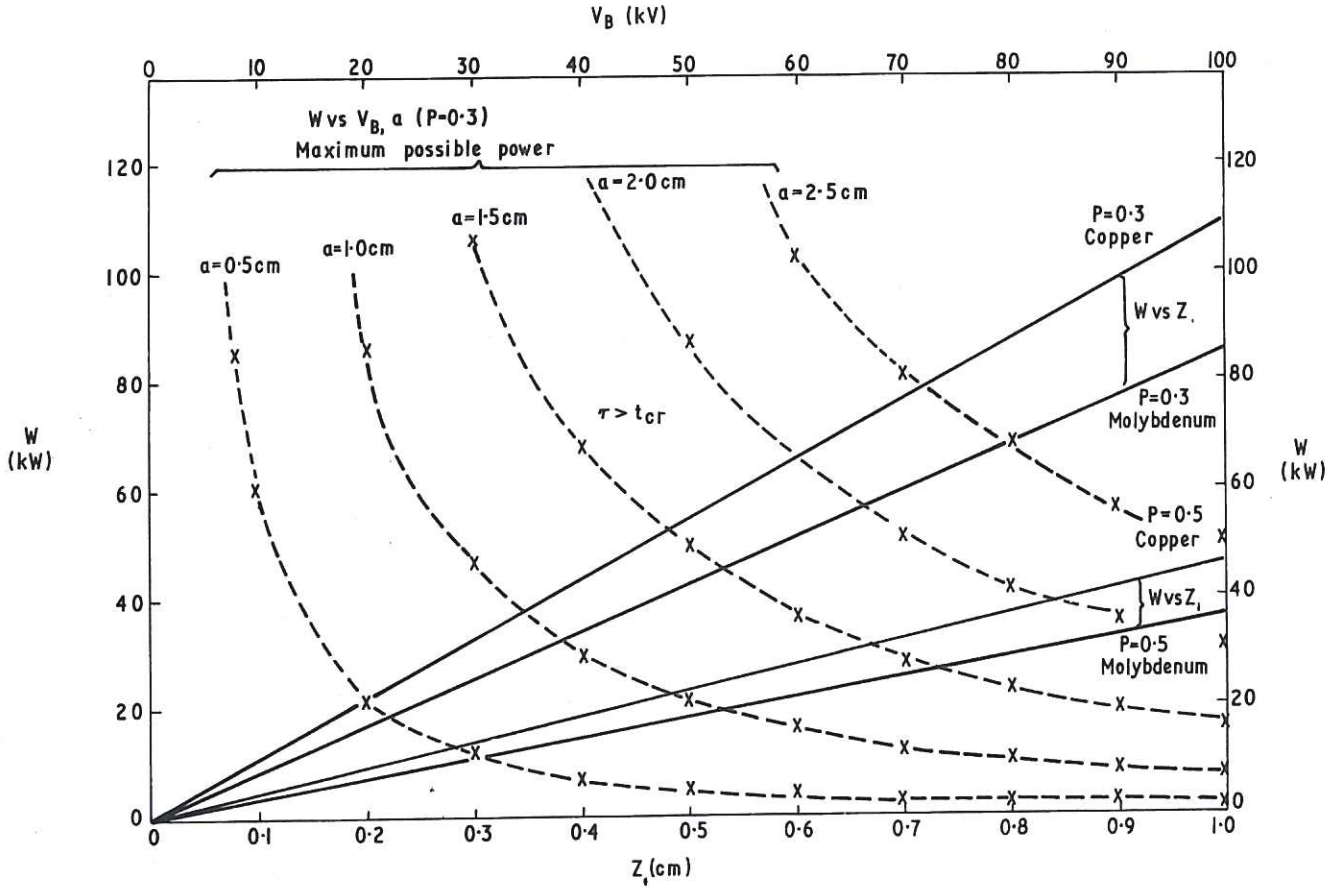

Fig. 8 The limitations on extracted power for $\tau < t_{cr}$ as a function of electrode thickness and breakdown voltage.

$$d_1 = \left(\frac{C_m P F \tau V_A^{\frac{5}{2}}}{4.2(1-P)\varepsilon \beta \rho^* C_v \Delta T_{cm}} \right)^{\frac{1}{3}} , \quad \text{for } V_A < V_B (d_1) \qquad ..(25)$$

$$\frac{W_m}{\pi a^2} = C_m P . V_A^{\frac{5}{8}} \left(\frac{4.2(1-P)\varepsilon \beta \rho^* C_v \Delta T_{cm}}{C_m P F \tau} \right)^{\frac{3}{8}} \qquad ..(26)$$

For our values for copper

$$\frac{W_m}{\pi a^2} \approx \left(\frac{0.28}{\tau} \right)^{\frac{3}{8}} V_A^{\frac{5}{8}} \text{ Watts/cm}^2 \leq \frac{C_m P B^4}{V_B^{\frac{3}{2}}} \qquad ..(27)$$

(e) In Fig.8 we plot W vs z_1 for the case $\tau > t_{cr}$ using equation (18) with the same values for ε, β, and F, and P = P.3 and 0.5. We also show the maximum possible power for various electrode radii taken from (24) and plotted as a function of V_B for P = 0.3. Again, at the lower voltages we can benefit from setting an extra large extraction gap with thicker electrodes because we are limited more by dissipation than by perveance. These dissipation calculations are combined with other results and are applied to ion source design in CLM P311.

Note

For copper $\rho C_v = 0.98$ cal cm^{-3} K^{-1} ,
$K = 0.9$ cal cm^{-1} sec^{-1} K^{-1}

For molybdenum $\rho C_v = 1.13$ cal cm^{-3} K^{-1}
$K = 0.3$ cal cm^{-1} sec^{-1} K^{-1} .

6. PROTECTION OF ELECTRODES

We have seen that the current drain on the negative electrode indicates the level of positive ion interception and is therefore a measure of the heat dissipation which is approximately $\frac{I_N V_A}{3}$ Watts. A simple protective device can be obtained by tapping a small percentage of this current and using it to feed an integrator of time constant $\sim t_{cr}$. A voltage sensing unit set at the level corresponding to that of the maximum permissible power dissipation could be used to trip out the power supplies in the event of an excessive load.

REFERENCES

1. Aldcroft, D., Burcham, J., Cole, H.C., Cowlin, M., Sheffield, J., CLM-P314, 1972.
2. Coupland, J., Green, T., Hammond, P., Riviere, A.C., CLM-P312, 1972.
3. Carslaw, H.S., Jaeger, J.C., Conduction of heat in solids. Oxford Clarendon Press 1959, p.204.
4. Davis, R.C., Morgan, O.B., Stewart, L.D., Stirling, W.L., Rev. Sci. Inst., 43, 278, 1972.